

This is the accepted manuscript version of the contribution published as:

Reino, C., Ding, C., Adrian, L. (2023):

Continuous cultivation of *Dehalococcoides mccartyi* with brominated tyrosine avoids toxic byproducts and gives tight reactor control. *Water Res.* **229** , art. 119396

The publisher's version is available at:

<http://dx.doi.org/10.1016/j.watres.2022.119396>

1 Continuous cultivation of *Dehalococcoides mccartyi* with 2 brominated tyrosine avoids toxic byproducts and gives tight 3 reactor control

4 Clara Reino¹, Chang Ding^{1,*}, Lorenz Adrian^{1,2}

5 ¹ Helmholtz Centre for Environmental Research – UFZ, Department of Environmental
6 Biotechnology, Permoserstraße 15, 04318 Leipzig, Germany

7 ² Chair of Geobiotechnology, Technische Universität Berlin, Ackerstraße 76, 13355 Berlin,
8 Germany

9

10 Running title: *Dehalococcoides* CSTR

11

12 *To whom correspondence should be addressed: Chang Ding, Helmholtz Centre for
13 Environmental Research – UFZ, Department of Environmental Biotechnology, Permoserstraße
14 15, 04318 Leipzig, Germany, Tel.: +49 341 235 1435, Fax: +49 341 235 1443, E-Mail:
15 chang.ding@ufz.de

16

17 Abstract

18 *Dehalococcoides mccartyi* strain CBDB1 is a strictly anaerobic organohalide-respiring
19 bacterium with strong application potential to remediate aquifers and soils contaminated with
20 halogenated aromatics. To date, cultivation of strain CBDB1 has mostly been done in bottles
21 or fed-batch reactors. Challenges with such systems include low biomass yield and difficulties
22 in controlling the growth conditions. Here, we report the cultivation of planktonic *D. mccartyi*
23 strain CBDB1 in a continuous stirring tank reactor (CSTR) that led to high cell densities
24 ($\sim 8 \times 10^8$ cells mL⁻¹) and dominance of strain CBDB1. The reactor culture received acetate,
25 hydrogen, and the brominated amino acid D- or L-3,5-dibromotyrosine as substrates. Both D-
26 and L-3,5-dibromotyrosine were utilized as respiratory electron acceptors and are promising
27 for biomass production due to their decent solubility in water and the formation of a non-toxic
28 debromination product, tyrosine. By monitoring headspace pressure decrease which is
29 indicative of hydrogen consumption, the organohalide respiration rate was followed in real
30 time. Proteomics analyses revealed that the reductive dehalogenase CbdbA238 was highly
31 expressed with both D- and L-3,5-dibromotyrosine, while other reductive dehalogenases
32 including those that were previously suggested to be constitutively expressed, were repressed.
33 Denaturing gradient gel electrophoresis (DGGE) of amplified 16S rRNA genes indicated that
34 the majority of cells in the community belonged to the *Dehalococcoides* although the CSTR
35 was operated under non-sterile conditions. Hence, tightly controlled CSTR cultivation of
36 *Dehalococcoides* opens novel options to improve biomass production for bioaugmentation and
37 for advanced biochemical studies.

38

39 **Keywords:** organohalide respiration; continuous stirred tank reactor; brominated phenolic
40 compounds; online activity monitoring; bioremediation

41 1 Introduction

42 Bacteria of the genus *Dehalococcoides* are being commercially used to remediate aquifers
43 contaminated with halogenated and highly persistent compounds, such as perchloroethene
44 (PCE) (Steffan and Schaefer, 2016). Various *Dehalococcoides* strains have been isolated which
45 are able to transform halogenated compounds including chlorinated dioxins, biphenyls (PCBs),
46 benzenes, anilines, and thiophenes (Zinder, 2016). In addition, brominated and iodinated
47 compounds such as brominated flame retardants and iodinated X-ray contrast media are
48 reductively dehalogenated. This reductive dehalogenation is coupled in *Dehalococcoides*
49 strains to energy conservation via a respiratory chain with hydrogen as an electron donor and
50 acetate plus carbonate as the carbon sources. No other mode of energy conservation than this
51 organohalide respiration has been detected in any of the isolated *Dehalococcoides* strain. On
52 one hand, this high physiological specificity is good for *in situ* application because the
53 occurrence of reductive dehalogenation can be tightly correlated with the presence of
54 *Dehalococcoides*. On the other hand, the physiological specificity also makes the production of
55 cell mass challenging: as a prerequisite, cell growth requires the presence of halogenated
56 compounds which often have low water solubility and are often toxic at concentrations in the
57 micromolar range. However, electron acceptors have to be added in the millimolar range to
58 obtain sufficient cell numbers because of the molar growth yield of about 10^{13} - 10^{14} cells per
59 mol of halogen substituent removed (Cooper et al., 2015). Such concentration of halogenated
60 compounds is difficult to achieve in batch cultures and often causes growth inhibition. Another
61 challenge in the cultivation of *Dehalococcoides* strains is the formation of less-halogenated
62 compounds as end products of the dehalogenation reaction that can be more toxic than the
63 parent compound. For example, many *Dehalococcoides* strains transform PCE only to the more
64 toxic intermediate vinyl chloride (VC) which accumulates in the cultivation broth. A third
65 challenge is the high oxygen sensitivity of *Dehalococcoides* strains that requires cultivation in
66 gas-tight vessels with oxygen-protection by reducing agents. A last complication in the
67 cultivation of *Dehalococcoides* strains is the monitoring of activity and cell growth, because no
68 detectable turbidity can be observed during bacterial growth due to the small size of the cells,
69 and offline monitoring of cell counts or compound concentrations is laborious. It is therefore
70 time-consuming to determine the optimum harvesting moment when the bacteria reach their
71 late exponential growth phase in a batch culture.

72 The genomes of all fully sequenced *Dehalococcoides* strains contain many different reductive
73 dehalogenase operons, most of which encode a catalytic subunit RdhA and a small ~90 amino
74 acid integral membrane protein RdhB which is assumed to be a membrane anchor for RdhA. In
75 our previous work we have shown that the two proteins RdhA/RdhB form a distinct module
76 which is part of a larger respiratory membrane-bound protein complex containing additionally
77 a central module (three different subunits of a complex iron-sulfur molybdoenzyme, CISM,
78 (Rothery et al., 2008)) and a hydrogen uptake module with a two-subunit, cytochrome-free
79 hydrogenase HupL/HupS (Kublik et al., 2016; Seidel et al., 2018). RdhA and RdhB have shown
80 to be inducible, and it is hypothesized that different RdhA/RdhB versions can be incorporated
81 into the respiratory complex. The inducibility of the RdhA/RdhB module is supported by the
82 almost invariable presence of the gene for a transcription regulator (two component systems or
83 MarR-type regulators) upstream of the promoter of rdh-operons and has also been demonstrated
84 by proteomic studies as a response to electron acceptor change (Franke et al., 2020; Yang et al.,
85 2015). This emphasizes that for successful application of *Dehalococcoides* cultures in
86 bioremediation not only the cell number and growth status are important but also the presence
87 of appropriate RdhA/RdhB proteins.

88 In contrast to batch cultivation, the use of CSTR as bioreactor for cultivation allows to establish
89 optimal cultivation conditions, by tightly controlling physicochemical parameters, such as pH,

90 redox potential or temperature. Cultivation in CSTR is also able to maintain the cell growth at
91 a specific growth rate (i.e., specific doubling time). Cultivation of *Dehalococcoides* species in
92 continuous or fed-batch reactors have been reported with PCE, trichloroethene (TCE), or VC
93 as electron acceptors (Mao et al., 2019; Mortan et al., 2017; Berggren et al., 2013; Delgado et
94 al., 2014; Richardson et al., 2002). Fermentable organic compounds such as lactate, pyruvate
95 or methanol were used as carbon source and electron donor, and therefore led to enrichment of
96 fermentative bacteria or methanogens and in many cases led to low abundance of
97 *Dehalococcoides* species (Berggren et al., 2013; Mao et al., 2019; Mortan et al., 2017). By
98 operating a continuous reactor at low hydraulic retention time (HRT, 3 d) and high TCE
99 concentration (1-2 mM), Delgado et al. (2014) achieved high cell densities of *Dehalococcoides*
100 ($>10^9$ cells mL⁻¹). In that study, lactate and methanol were fed and *Geobacter* as well as
101 methanogenic archaea were detected. With high flow rate in the reactor, dominance of
102 *Dehalococcoides* could be achieved. Concerns were raised on the accumulation of inhibitory
103 volatile compounds (e.g., carbon monoxide) in the headspace in continuous reactors during the
104 cultivation of *Dehalococcoides* (Mortan et al., 2017; Zhuang et al., 2014), but such inhibition
105 was not observed in the study by Delgado et al. (2014).

106 In our study, we attempted to cultivate *Dehalococcoides* without fermentable substrates. The
107 reactor medium contained acetate as an organic carbon source and hydrogen was added in the
108 reactor headspace as the electron donor. Cultivation without fermentable substrates has two
109 advantages: 1) it guarantees that *Dehalococcoides* will become the dominant species in the
110 reactor since fermentative bacteria cannot thrive, 2) it enables online monitoring of
111 dehalogenation activity through pressure drop caused by H₂ consumption. A novel electron
112 acceptor, D- or L-3,5-dibrominated tyrosine, that can be reductively debrominated to the non-
113 toxic debromination product, tyrosine, was introduced in this study. By setting up continuous
114 cultivation in a CSTR, we aimed to assess the feasibility of a reliable and on-line monitored
115 cultivation of *D. mccartyi* strain CBDB1, with acetate as the carbon source, and hydrogen in
116 the headspace as the electron donor. Growth and dehalogenation were evaluated in regard to
117 process stability and biomass yield. The presented reactor system has potential applications not
118 only for the large-scale generation of highly active cell biomass of *D. mccartyi* for *in-situ*
119 applications but also for the production of cell biomass for biochemical research.

120 **2 Material and Methods**

121 **2.1 Synthetic medium used for cultivation**

122 A synthetic medium was used for cultivation as influent of the semi-continuous stirred tank
123 reactor. This medium was pH-buffered with 10 mM bicarbonate, reduced with 2 mM cysteine
124 and amended with 5 mM acetate as a carbon source. It also contained a mixture of the vitamins
125 biotin, thiamine, cyanocobinamide and dimethylbenzimidazole, apart from basic minerals and
126 trace metals as described before (Adrian et al., 1998; Schipp et al., 2013). The synthetic medium
127 was amended with D- or L-3,5-dibromotyrosine (abcr Chemie, Karlsruhe, Germany) depending
128 on the type of cultivation performed. For cultivation in batch, starting concentrations between
129 0.5 and 4 mM of D-3,5-dibromotyrosine (D-DBT) were used; for setting up the CSTR, the
130 synthetic medium used as influent was amended with 5 mM final concentration of D-DBT and
131 later on, the reactor started operation using the synthetic medium amended with either 5 mM or
132 1 mM final concentration of L-3,5-dibromotyrosine (L-DBT) depending on the period of
133 operation. The change from D-DBT to L-DBT was made due to the suitability of both isomers
134 for the cultivation purposes and the much lower cost of L-DBT compared to D-DBT.

135 2.2 Reactor setup

136 The principles of the reactor setup have been described in a previous work for the cultivation
137 of the anammox bacterium “*Candidatus* Kuenenia stuttgartiensis” (Ding et al., 2018). The
138 reactor was gas-tight and contained sealed ports to connect a temperature probe and for adding
139 medium and sampling through septa (Figure S1). Continuous operation of the reactor was
140 enabled with an automated PSD/4 syringe pump (Hamilton, Bonaduz, Switzerland) equipped
141 with a 5-mL syringe (model 1010.5 TLL with plunger made of ultra-high-molecular-weight
142 polyethylene) and a six-port distribution valve (Hamilton, Bonaduz, Switzerland). By switching
143 the valve to one of the six ports, the syringe pump could perform multiple alternative actions
144 such as adding fresh medium / H₂ and removing reactor liquid. In programmed frequency as
145 calculated based on the targeted hydraulic retention time (HRT), the syringe pump withdrew a
146 fixed volume of reactor liquid (<2% of reactor volume) and added the same volume of fresh
147 medium. The operation was controlled and monitored via a Raspberry Pi microprocessor
148 running a self-developed Python script. The Raspberry Pi was also used to continuously monitor
149 the gas pressure in the reactor headspace from a simple pressure sensor (MPX5100DP, NXP
150 Semiconductors). In our study, two lab-scale continuous stirred tank reactors were used for
151 cultivation. The first reactor had a volume of 1 liter and was used during Periods I and II of
152 operation. pH values were regularly monitored offline by withdrawing samples for
153 measurement, and adjustment of pH in the reactor liquid was done with 5 M NaOH. Throughout
154 the reactor operation period, the pH was maintained at 6.8 ± 0.4 .

155 2.3 Microbiological techniques

156 Samples for cell counting were withdrawn from the reactor with a sterile plastic syringe. When
157 necessary, samples were diluted in MilliQ water before staining. Cells were quantified by direct
158 cell counting on agarose-coated slides with an epifluorescence microscope after staining with
159 SYBR-Green as described previously (Marco-Urrea et al., 2011). This method has a
160 quantification limit of about 10^6 cells mL⁻¹.

161 Samples for DNA extraction were withdrawn from the reactor with a sterile plastic syringe and
162 pelleted by centrifugation (twice at 14,000 g, 16 °C, 30 min). The resulting pellet was used for
163 extraction of genomic DNA by using the NucleoSpin Tissue kit (Macherey-Nagel) according
164 to the manufacturer’s instructions. PCR amplification of 16S rRNA genes was done using the
165 GC-clamped forward primer 341FGC 5’-CGC CCG CCG CGC GCG GCG GGC GGG GCG
166 GGG GCA CGG GGGG CCT ACG GGA GGC WGC AG- 3’ and the reverse primer 518R12
167 5’-WTT ACC GCG GCT GCT GG-3’. The PCR products were checked on 1% agarose gels
168 and subjected to denaturing gradient gel electrophoresis (DGGE) using the DCode Universal
169 Mutation Detection System (Bio-Rad). Gels were prepared at 10% polyacrylamide and a
170 gradient of 20-80% denaturing agents, where 100% corresponds to 7 M urea and 32% v/v
171 formamide. Amplified PCR products of 12 µL were loaded onto the gel and electrophoresis
172 was run in 1× TAE buffer at 100 V and 60 °C for 16 h. The gel was SYBR-Gold stained, the
173 bands were cut and DNA was eluted by overnight incubation in 10 mM Tris·HCl at pH 8.5.
174 The eluted DNA was PCR amplified again (primers 341FGC-518R12), and the PCR products
175 were purified and sent for Sanger sequencing (Eurofins Genomics Europe). The sequencing
176 results were used for taxonomic identification by matching against the NCBI nt database using
177 nucleotide BLAST (<http://www.ncbi.nlm.nih.gov/BLAST/>).

178 2.4 Ion chromatography, liquid chromatography, and shot-gun proteomics analyses

179 Samples from the reactor were periodically withdrawn for further analyses. The bromide ion
180 concentration was quantified via ion chromatography using a Dionex-120 ion chromatograph
181 equipped with an IonPac AS4A-SC (4 mm × 250 mm) column (detection limit: 10 µM).

182 Dibromotyrosine, bromotyrosine and tyrosine were analyzed by means of a high-performance
 183 liquid chromatography (HPLC) system with a LiChrospher 100 RP-18 (5 μm) LiChroCART
 184 125-4 column with methanol and 0.1% formic acid as the mobile phase. Before HPLC analysis,
 185 primary amine groups in samples were derivatized using diethyl ethoxymethylenemalonate
 186 (DEEMM). To do this, 200 μL of sample was added into 1 mL of reaction buffer containing
 187 7:3 v/v mixture of 50 mM borate buffer (pH 9) and methanol. Then 6 μL of DEEMM was added
 188 and the derivatization was carried out overnight at room temperature in the dark. The
 189 derivatized tyrosine and brominated tyrosines were detected in the HPLC at a wavelength of
 190 280 nm (detection limit: 5 μM). For shot-gun proteomics, 1 mL of reactor liquid was centrifuged
 191 down at 14,000 g, 16 °C, 30 min to obtain the cell pellet. Cell disruption, trypsin digestion, and
 192 peptide desalting using C₁₈ ziptips (Millipore, Merck) were done as previously described (Ding
 193 and Adrian, 2020). Desalted peptides were analyzed using nano-liquid chromatography coupled
 194 to tandem mass spectrometry (nLC-MS/MS) with an Orbitrap Fusion (Thermo), under the
 195 analytical conditions described before (Ding and Adrian, 2020). Mass spectra were evaluated
 196 with ProteomeDiscoverer software v2.4 (Thermo) and protein quantities were calculated by
 197 using the peak areas of precursor peptides in the MS1 scans using the Minora node of
 198 ProteomeDiscoverer. To calculate relative abundances (%), the abundance of a target protein
 199 was divided by the sum of abundances of all detected proteins in a sample.

200 2.5 Calculations

201 As shown in Equation 1, in a chemostat the dilution rate (D) is equal to the growth rate (μ) of
 202 the culture and the inverse of the hydraulic retention time (HRT). Therefore, the growth rate
 203 can be modified by changing the inflow rate (F) or the liquid volume of the reactor (V).

$$204 \mu = D = \frac{1}{HRT} = \frac{F}{V} \quad \text{(Equation 1)}$$

205 The hydraulic loading rate was calculated as the molar amount of DBT entering the system per
 206 units of volume in the reactor per day of operation, and the specific loading rate was calculated
 207 as the molar amount of DBT entering the system per bacterial cell in the reactor per day of
 208 operation. These design parameters were calculated as follows:

$$210 \text{Hydraulic Loading Rate} \left(\frac{\text{mmol DBT}}{\text{L} \cdot \text{day}} \right) = \frac{[\text{DBT}]_{\text{influent}} \left(\frac{\text{mmol}}{\text{L}} \right) \times F \left(\frac{\text{L}}{\text{day}} \right)}{V(\text{L})} \quad \text{(Equation 2)}$$

211 where, [DBT]_{influent} is the concentration of L-DBT in the influent (1 mM or 5 mM depending
 212 on the period of operation); F is the inflow rate applied in the CSTR and V is the liquid volume
 213 of the CSTR (1 L or 80 mL depending on the period of operation)
 214

$$216 \text{Specific Loading rate} \left(\frac{\text{mmol DBT}}{\text{cell} \cdot \text{day}} \right) = \frac{\text{Hydraulic Loading Rate} \left(\frac{\text{mmol DBT}}{\text{L} \cdot \text{day}} \right)}{[\text{cells}]_{\text{reactor}} \left(\frac{\text{cells}}{\text{L}} \right)} \quad \text{(Equation 3)}$$

217 where, [cells]_{reactor} is the cell density of the culture in the CSTR
 218

220 The molar growth yield was calculated considering the steady state operation as follows:

$$221 \text{Molar Growth Yield} \left(\frac{\text{cell}}{\text{mol Br}^-} \right) = \frac{[\text{cells}]_{\text{effluent}} \left(\frac{\text{cells}}{\text{L}} \right)}{[\text{DBT}]_{\text{influent}} \left(\frac{\text{mol DBT}}{\text{L}} \right) \times SR \left(\frac{\text{mol Br}^-}{\text{mol DBT}} \right)} \quad \text{(Equation 4)}$$

222

223 where, $[\text{cell}]_{\text{effluent}}$ is the cell density of the effluent in the CSTR, which is equal to the cell
224 density of the culture; $[\text{DBT}]_{\text{influent}}$ is the influent concentration of L-DBT (1 mM or 5 mM
225 depending on the period of operation); SR is the stoichiometry ratio of the dehalogenation
226 reaction of the dibromotyrosine, i.e., SR is equal to 2 mol bromide released per mol of
227 dibromotyrosine dehalogenated.

228 3 Results

229 3.1 Debromination of 3,5-dibromotyrosine by *D. mccartyi* strain CBDB1

230 In preliminary experiments with batch cultures, it was shown that *D. mccartyi* strain CBDB1
231 can use D-DBT as a terminal electron acceptor and can grow on the basis of this reaction
232 through anaerobic respiration with acetate plus carbonate as the carbon source and hydrogen as
233 the electron donor (results not shown). Initial concentrations in the cultures between 0.5 and
234 4 mM of D-DBT were tested in batch cultures and growth was shown by direct cell counting,
235 however complete inhibition of cell growth was observed with 4 mM of D-DBT. The maximum
236 cell density obtained in these batch cultures was 1.0×10^8 cell mL⁻¹. The products of the D-DBT
237 dehalogenation process were tyrosine and bromide, and the results matched the theoretical
238 stoichiometry of 1:2 dibromotyrosine:bromide.

239 3.2 Start-up of continuous cultivation of strain CBDB1 in a CSTR

240 A pre-reactor was set up to produce active culture liquid for the inoculation of the main reactor.
241 The pre-reactor vessel contained 950 mL cysteine-reduced medium with 1 mM D-DBT and
242 was inoculated with 50 mL active culture containing 5.0×10^7 mL⁻¹ *D. mccartyi* strain CBDB1
243 which was previously growing on 1 mM D-DBT in serum bottles. At day 0 of the pre-reactor
244 operation, 6.7 kPa of H₂ were added into the headspace as the electron donor, and H₂ was
245 regularly replenished when the pressure dropped. On day 11 of pre-reactor operation, cell
246 density reached 1.7×10^7 cells mL⁻¹ and the concentration of bromide ions (as determined by ion
247 chromatography, see below) reached 1.6 mM. Then, the pre-reactor headspace was periodically
248 flushed with H₂ and a small share of the pre-reactor liquid was periodically replaced with fresh
249 medium containing 5 mM of D-DBT, with a maximum single dose of 50 mL (resulting in a
250 concentration increase of 0.25 mM D-DBT in the pre-reactor). On day 21 of pre-reactor
251 operation, the cell density reached 1.4×10^8 cell mL⁻¹ and the bromide concentration reached 6.8
252 mM. Then, the pre-reactor was switched to a daily flow of 43.2 mL, equivalent to an HRT of
253 23 d. Such reactor flow was maintained for 23 days and 1 L of effluent was captured and stored
254 at 4.5 °C. After one-month storage at 4.5 °C, the effluent was filtered through wide-pore filter
255 paper under strictly anoxic conditions in the anaerobic tent to remove tyrosine crystals. The
256 filtrate was transferred into the clean reactor vessel as the starting reactor liquid (day 0 of the
257 main reactor). With the beginning of the main reactor operation, the electron acceptor was
258 switched from 5 mM D-DBT to 5 mM L-DBT, while the HRT remained at 23 d.

259 On day 57, 16 mL of reactor liquid was mixed anoxically with 64 mL fresh medium containing
260 no DBT as the starting reactor liquid for a downscaled 80-mL reactor. The reduction in reactor
261 volume was decided in order to achieve higher daily flows in the reactor without stressing the
262 syringe pump. For this 80-mL reactor, the concentration of L-DBT in the medium used as
263 influent was lowered from 5 mM to 1 mM. Lowering the DBT concentration at the high flow
264 rate was necessary because hydrogen transfer from headspace might have become limiting if
265 the DBT concentration in the medium was too high. On day 60 (3 days after the 80-mL reactor
266 was established), the continuous feeding of the CSTR was restarted.

267 3.3 Performance of the CSTR with a *D. mccartyi* strain CBDB1 enriched culture

268 The above-mentioned lab-scale CSTR (main reactor) was operated in continuous mode for 155
269 days with L-DBT as the electron acceptor. The operation was divided into six periods (I to VI)
270 based on different hydraulic conditions applied to the reactor. The dilution rate was stepwise
271 increased to achieve fast growth. Thus, the HRT was decreased from 23 days in Period I to 4
272 days in Period VI (Figure 1). Successful continuous reactor operation was achieved without
273 accumulation of brominated compounds and the results again accorded to the theoretical molar
274 stoichiometry of 1:2 dibromotyrosine:bromide ions. Decrease of reactor headspace pressure
275 was constantly observed, indicating H₂ consumption.

276 Figure 1 shows the L-DBT loading rate and the L-DBT specific removal activity achieved for
277 each period of operation. The specific removal activity was not plotted for Period I because the
278 reactor had not reached the pseudo steady state yet. Still, the measured values of L-DBT
279 concentration were very low during this period. In fact, the concentration of L-DBT in the
280 reactor was under the detection limit (5 μM) during most of the operation time. The same was
281 true for the potential dehalogenation intermediate 3-monobromotyrosine. Accumulation of L-
282 DBT was only observed during the start-up of the continuous operation (Period I), with 0.03,
283 0.02, 1.3 and 0.02 mM of L-DBT measured on days 1, 8, 17 and 28, respectively, indicating
284 that the culture had to adapt to the conditions during Period I. The highest L-DBT concentration
285 was detected on day 17 which was due to the restart of the operation after one day of starving
286 conditions (fresh medium input was stopped for one day). For the rest of the operation, we did
287 not again observe a significant increase of L-DBT in the reactor, indicating that the bacterial
288 growth was continuously limited by the concentration of L-DBT. From Period II to IV, the
289 removal rate was maintained at an average value of $7 \times 10^{-12} \pm 3 \times 10^{-12}$ nkat cell⁻¹. It is important
290 to notice that, when the hydraulic loading rate decreased from Period II to III, the specific
291 loading rate (i.e., the amount of L-DBT loaded per cell) was still maintained. This is due to the
292 fact that chemostat operations allow for uncoupling of the growth rate and the cell density of
293 the culture, and here both parameters changed when moving from Period II to III (higher μ and
294 lower electron acceptor concentration in the influent were applied, resulting in an unchanged
295 specific loading rate). In Periods V and VI, the L-DBT specific loading rate was increased and
296 no increase of the L-DBT concentration was observed in the reactor liquid. The average specific
297 removal rate achieved during Period V and beginning of Period VI was $2.5 \times 10^{-11} \pm 0.5 \times 10^{-11}$
298 nkat cell⁻¹. On day 149, the L-DBT loading rate was further increased to 6.1×10^{-12} mmol DBT
299 cell⁻¹ day⁻¹ and again no accumulation of brominated compounds occurred.

300 During Periods I and II, the formation of whitish turbidity was observed in the reactor, but the
301 operation was not affected. Under these circumstances, when the effluent of the reactor was
302 collected and stored at 4.5 °C, the formation of needle-like crystals occurred, while the
303 supernatant was clear (Figure S2). Since the tyrosine concentration in the CSTR (5 mM) was
304 higher than the tyrosine solubility in water (2.5 mM), the precipitates were expected to be
305 tyrosine crystals, which was the final product of the debromination process from L-DBT. The
306 identity of the crystals was confirmed with HPLC-UV by comparing to the retention time and
307 absorbance spectra of a neat tyrosine standard.

308 The continuous cultivation in the CSTR allowed for the calculation of H₂ consumption based
309 on the decrease of pressure in the reactor headspace. Periodically, the actual gas consumption
310 was calculated from the pressure data and it matched with the theoretical values expected from
311 the molar stoichiometry of 1:2 dibromotyrosine:hydrogen (Figure 2, Table 1). Hence, the extent
312 of the dehalogenation process of L-DBT was assessed in real-time during the entire operation
313 of the CSTR. For instance, on day 17, when the medium feeding was stopped, no decrease in
314 headspace pressure was observed (i.e., no consumption of H₂).

315 The cell density obtained in the CSTR varied according to the operation conditions (Figure 3)
316 and the maximum cell density achieved was of 8.5×10^8 cell mL⁻¹, only limited by the L-DBT
317 concentration. The decrease of cell density observed from Period II to III was related to the
318 decrease of L-DBT concentration in the influent from 5 mM to 1 mM, and the decrease of cell
319 density observed from Period IV to V was due to a culture withdrawn intentionally, performed
320 during sampling.

321 The molar growth yield of the culture growing on L-DBT varied during the different periods of
322 cultivation, resulting in $9 \times 10^{13} \pm 5 \times 10^{13}$ cell mol⁻¹ Br⁻. The highest molar growth yield was
323 obtained on Periods III and IV, with an average value of $1.2 \times 10^{14} \pm 0.3 \times 10^{14}$ cell mol⁻¹ Br⁻.
324 Under the same conditions of electron acceptor influent concentration (Periods III to VI, 1 mM
325 of 3,5-DBT), the higher the growth rate imposed (i.e., the younger the culture), the lower the
326 molar growth yield observed (Figure 4).

327 Figure 5 shows an image of the SYBR green stained cells withdrawn from the CSTR and the
328 results of one of the DGGE analyses performed on a culture sample. On one hand, during the
329 entire operation the typical spherical cell shape of *D. mccartyi* strain CBDB1 was observed in
330 samples directly withdrawn from the CSTR. On the other hand, DGGE results demonstrated
331 that a high enrichment in *D. mccartyi* strain CBDB1 was maintained when operating the CSTR,
332 despite the reactor was not operated under sterile conditions.

333 3.4 Expression of reductive dehalogenases

334 Samples of the CSTR culture were periodically withdrawn to evaluate the expression of
335 reductive dehalogenases. Shotgun proteomics analyses were performed with samples of days
336 8, 21, 57, 112 and 144, all from culture growing on L-DBT. A sample from the culture growing
337 on D-DBT in the pre-reactor (see Section 2.2 for details) was also used for shotgun proteomics
338 for comparison. A total of nine different RdhA proteins were identified to be expressed,
339 although not in all the periods of operation (Table 2, Table S1). The relative abundance of the
340 different RdhA also varied among periods. CbdbA84, CbdbA238 and CbdbA1092 were
341 identified in all the samples, although no correlation with time of operation and relative
342 abundance was observed. Overall, CbdbA238 and CbdbA1092 showed the highest abundance
343 compared to the other RdhA identified in the samples, with the exception of sample from Period
344 IV, when CbdbA84 was also highly expressed. Details on the protein abundances can be found
345 in the Supplementary Material.

346 A cross-comparison of RdhA abundance among CBDB1 culture fed with different halogenated
347 compounds (Table 2) showed an association of expressed RdhA with the type of halogenated
348 compound added: CbdbA80 and CbdbA84 were highly expressed when halogenated benzenes
349 were provided, whereas CbdbA1092 was only detected when the halogenated compound
350 contained a phenol ring (DBT, tetrabromobisphenol A, or bromophenol blue). The expression
351 of CbdbA238 was exclusively associated with culture fed with L- or D-DBT, indicating specific
352 induction by this compound. A significant difference between the induction by L- and D-DBT
353 was not found.

354 4 Discussion

355 4.1 CSTR as a strategy for cultivating *Dehalococcoides*

356 The results of this study show how *D. mccartyi* strain CBDB1 can be cultivated in continuous
357 mode in a CSTR using L-DBT as electron acceptor, hydrogen as electron donor and acetate as
358 carbon source. The CSTR design used here was introduced in a previous work of the authors
359 as a very useful tool to cultivate anammox bacteria (Ding et al., 2018), but it was not tested so

360 far for anaerobic cultivation where a substrate was added from the gaseous phase. This is an
361 important issue when cultivating the strictly anaerobic bacteria *D. mccartyi* strain CBDB1
362 because potential negative headspace pressure could lead to air leakage, which would trigger
363 the cessation of the dehalogenation process. The gas-sealed setup, the continuous monitoring
364 of pressure in the headspace and the automated maintenance of a positive pressure in the gas
365 phase allowed for a successful long-term stable operation of the CSTR, demonstrating the
366 feasibility of using the CSTR for cultivation under anoxic conditions. Besides, the continuous
367 monitoring of headspace pressure allowed the quantitative evaluation of the dehalogenation
368 process in real-time because the rate of pressure decrease quantitatively correlated with the L-
369 DBT consumption rate. Such precise online monitoring is key for controlling the
370 dehalogenation process in continuous mode in CSTR. In addition, the CSTR operation provided
371 robustness to face changing loading rates. As shown in Figure 1, L-DBT concentration in the
372 CSTR was zero even when the specific loading rate was increased from day 120 onwards. The
373 increase in removal rate without any accumulation of L-DBT indicated that the culture growth
374 was limited by a lack of the halogenated electron acceptor. Hence, the *D. mccartyi* strain
375 CBDB1 culture was not yet at its maximum dehalogenation capacity. In general, cultivation in
376 continuous mode can achieve higher dehalogenating rates than in batch mode, because the
377 continuous mode maintains the bacteria in their exponential growth phase. This is best
378 illustrated by the accumulation of dibromotyrosine on day 17 after starving the reactor for only
379 one day (Figure 1), showing cells that have been starved for only one day were not able to cope
380 with the loading rate that was applied before. The dehalogenation rates obtained in this study
381 are in the same range of those reported by Delgado et al. (2014) for dichloroethene
382 dehalogenation in a CSTR containing a *Dehalococcoides* dechlorinating mixed-culture (0.5-1.4
383 mmol Cl⁻¹ d⁻¹).

384 Another important advantage of the CSTR design is the possibility to control the cell density
385 of the culture by increasing the substrate concentration in the influent (Madigan et al., 2006).
386 Figure 3 shows that the highest cell density in the CSTR was obtained when the influent
387 concentration was 5 mM L-DBT. As expected in a chemostat, the higher the electron acceptor
388 concentration in the influent the higher the cell density of the culture. In this period, the steady
389 state was probably not achieved due to the high HRT applied (HRT of 23 and 17 days in Periods
390 I and II, respectively), and thus the maximum cell density was not achieved. Higher cell
391 numbers would be expected if there were no limitations in growth by lack of electron acceptor
392 and/or if higher influent concentrations than 5 mM were used. In this sense, the cultivation in a
393 CSTR allows the use of higher concentrations of electron acceptor than the ones used in batch
394 systems, because of the immediate dilution of influent when entering the reactor, overcoming
395 the potential toxicity or inhibition by electron acceptor addition. We observed complete
396 inhibition of the growth of *D. mccartyi* strain CBDB1 in batch cultures when using initial
397 concentration of 4 mM D-DBT, whereas 5 mM inflow concentration generated no problem in
398 the CSTR of this study. Despite the observed electron acceptor limitations, the bacterial growth
399 was sustained in the long-term in our CSTR, even when imposing a high inflow rate in the
400 system with a doubling time of 3 days in Period VI (*D. mccartyi* strain CBDB1 was reported to
401 have a doubling time between 1 and 3 days (Löffler et al., 2013)). Also, the maximum cell
402 density achieved in the CSTR cultivation (8.5×10^8 cell mL⁻¹) was higher than the usually
403 achieved maximum cell number in batch cultures ($1-5 \times 10^8$ cells mL⁻¹ in a fully-grown
404 culture). The feasibility of obtaining high cell density *D. mccartyi* strain CBDB1 cultures in
405 continuous mode makes the CSTR configuration a promising choice for establishing
406 bioremediation strategies for contaminated sites where a continuous feeding of high cell number
407 cultures with high activity are needed.

408 **4.2 3,5-dibromotyrosine as suitable electron acceptor for *D. mccartyi* strain CBDB1**

409 The cultivation of *D. mccartyi* strain CBDB1 using 3,5-dibromotyrosine was introduced here
410 for the first time and it was demonstrated that strain CBDB1 grows with both isomers D- and
411 L- of dibromotyrosine as electron acceptors. The brominated version of the amino acid tyrosine
412 was selected on the basis of its presumed harmlessness and its decent water solubility (10 mM
413 at room temperature), so its use for routine cultivation was considered to be picture-perfect: the
414 final product of its dehalogenation is non-toxic and does not contain any halogen substituent
415 anymore, so that the waste disposal is easy to handle in the laboratory. Altogether, this
416 organohalide is presented as promising electron acceptor to be used for cultivation purposes of
417 *D. mccartyi* strain CBDB1. In this study, growth of *D. mccartyi* strain CBDB1 was shown when
418 using both 5 mM and 1 mM of L-DBT, which represent very high concentrations in the
419 haloaromatics dehalogenation field. In comparison, with other brominated organic compounds,
420 concentrations in the micromolar range have often to be used to avoid toxicity and to observe
421 growth (Wagner et al., 2012; Yang et al., 2015). Hence, the possibility of using concentrations
422 as high as 5 mM is beneficial in terms of achieving high biomass concentrations for
423 bioremediation purposes. The potential limitation of the use of high concentrations of 3,5-DBT
424 as electron acceptor was the formation of precipitates of the final product, tyrosine, which could
425 trigger mass transfer problems in the reactor. This issue is addressed in the Section 4.3 below.

426 Full debromination of 3,5-DBT to the non-halogenated product and the associated growth of
427 strain CBDB1 was observed. The obtained molar growth yield ($9 \times 10^{13} \pm 5 \times 10^{13}$ cell mol⁻¹ Br)
428 was in the range of molar growth yields reported for *D. mccartyi* strain CBDB1 growing with
429 other brominated or chlorinated electron acceptors, such as bromobenzenes (1.8 to 2.8×10^{14}
430 cell mol⁻¹ Br (Wagner et al., 2012)), bromophenols (3×10^{14} (Yang et al., 2015)), chlorobenzenes
431 (7×10^{13} to 1×10^{14} cell mol⁻¹ Cl (Jayachandran et al., 2003)) or chlorophenols (8×10^{13} cell mol⁻¹
432 Cl (Adrian et al., 2007a)). All these reported molar growth yields were determined in batch
433 cultures and, thus, the molar growth yield was an integrated value over the whole incubation
434 period including all the different growth phases of batch cultivation. Here, we induced different
435 stable growth rates (cell doubling times) by changing the inflow rate and found that the molar
436 growth yield was lower when the growth rate was increased, i.e., when doubling time decreased
437 (Figure 4). Such decrease in molar growth yields at high growth rate is counterintuitive, as less
438 maintenance energy is spent when cells grow faster and should have led to higher molar growth
439 yields. Multiple reasons could have caused such a phenomenon: 1) it could be that with
440 increased inflow rate, cells detected higher availability of halogenated compounds and
441 expressed more respiratory proteins (Table S1), leading to more energy spent on each cell
442 division; 2) generally higher protein and DNA content and larger cell size in fast-growing cells;
443 3) biofilm may have accumulated on the reactor vessel, leading to lower cell molar growth
444 yields as calculated based on numbers of planktonic cells in reactor liquid, although we did not
445 observe visible biofilm formation. However, the maintenance energy requirements seemed to
446 play an inferior role. Further investigation is needed to elucidate the possible causes.

447 L- and D-DBT are not obvious natural substrates widely present in the environment to support
448 growth of *Dehalococcoides* species, but can still be respired by strain CBDB1. Similar
449 phenomena have been observed with other halogenated compounds that are used by strain
450 CBDB1 for anaerobic respiration, e.g., with bromophenol blue. Also, strain CBDB1 did not
451 encounter any brominated tyrosine since its transfer to continuous lab cultivation in 1995 and
452 there was no difference in the growth between the two DBT isomers. This all supports previous
453 conclusion that the reductive dehalogenases must react relatively unspecific towards a range of
454 halogenated aromatics (Cooper et al., 2015). Evidence accumulates that the side groups but not
455 the halogen substituents determine the specificity of reductive dehalogenases in
456 *Dehalococcoides*.

457 The stoichiometric conversion of hydrogen and DBT to tyrosine and the absence of any other
458 electron acceptors or fermentable substrates demonstrated that strain CBDB1 was using DBT
459 as a respiratory electron acceptor. The specific expression of RdhA proteins in cells withdrawn
460 from the CSTR indicated their involvement in this process. *D. mccartyi* strain CBDB1 contains
461 32 different reductive dehalogenase operons on the genome, each constituted by one *rdhA* and
462 one *rdhB* gene (plus regulatory genes) which encode the catalytic enzyme RdhA and its putative
463 membrane anchor RdhB. However, so far no clear correlation was established between the
464 transcription of these *rdhA* genes and the exposure to particular organohalides, and it was
465 suggested that a low and steady transcription of most of them occurs (Maillard and Willemin,
466 2019). Our results contribute to this idea since up to 9 different RdhA proteins were identified
467 but only two proteins were present with high abundances in all the samples collected from the
468 reactor. This fact suggests that those two proteins actually catalyzed the debromination of
469 dibromotyrosine. On one hand, we observed the specific induction of the RdhA protein
470 CbdbA238 which was not identified with previous halogenated electron acceptors, suggesting
471 specificity for reduction of dibromotyrosine. On the other hand, the high expression of
472 CbdbA1092 supports the hypothesis that this protein could be involved in the dehalogenation
473 of brominated oligocyclic phenolic compounds, as previously suggested by Yang et al. (2015)
474 when cultivating strain CBDB1 with bromophenol blue as electron acceptor. In fact,
475 unpublished results from our lab showed that CbdbA1092 was the only RdhA identified in
476 batch cultures when cultivating strain CBDB1 on bromophenol blue after five passages to fresh
477 medium (Table 2).

478 The RdhA CbdbA84, often identified in cultures of strain CBDB1, was identified in this study
479 in all the samples, although with significant abundance only at the end of the operation. This
480 RdhA was initially associated with the dehalogenation of chlorinated benzenes (Adrian et al.,
481 2007b), and it was also identified in the presence of brominated benzenes (Wagner et al., 2012).
482 It is worth to notice the disappearance of the reductive dehalogenase CbdbA80 commonly
483 found in protein samples of strain CBDB1 cultures, which could indicate that this RdhA is not
484 broadly expressed as it was thought and, more specifically, CbdbA80 is not specific for
485 dehalogenation of dibromotyrosine.

486 **4.3 Practical implications for the design of bioremediation strategies**

487 The stable and easily-maintainable operation, the resilience to face high loading rates, the
488 possibility of controlling cell density and maintaining the exponential phase of growth, and the
489 capacity of overcoming electron acceptor toxicity issues, make the CSTR design a promising
490 tool for producing cells of *D. mccartyi* strain CBDB1 for downstream applications. The CSTR
491 allows the control of the growth rate and the cell number independently. For producing biomass
492 at a maximum and stable cell density for full-scale applications of bioremediation, it will be of
493 paramount importance to determine (i) the optimum growth rate of the culture under the reactor
494 conditions and (ii) the optimum influent concentration of the electron acceptor that can be
495 handled. In addition, the success on growing an active culture using 3,5-dibromotyrosine that
496 produces non-toxic tyrosine makes the tandem CSTR-DBT the perfect choice to produce high
497 biomass concentrations of *D. mccartyi* strain CBDB1 for downstream processes, either
498 bioremediation processes or research experiments. The only potential drawback of using 3,5-
499 dibromotyrosine as electron acceptor is the relatively low water solubility of the end product of
500 the dehalogenation, tyrosine, since at concentrations higher than 2 mM it can already trigger
501 the formation of precipitates in the reactor. This precipitate formation could be a suitable
502 surface for biofilm formation and aggregations of bacteria could lead to mass transfer
503 limitations which limit the *D. mccartyi* strain CBDB1 growth. However, in this study such
504 limitations were not observed despite of the formation of precipitates during Periods I and II.
505 On the contrary, the precipitation of tyrosine allowed for an easy separation of it, and thus its

506 removal from the effluent by filtration. Hence, the precipitation of tyrosine could also be seen
507 as beneficial to obtain a clean effluent. Also, tyrosine is a natural compound that, although it is
508 not incorporated into the metabolism from external sources by strain CBDB1 (Marco-Urrea et
509 al., 2012) it can be used by many bacteria as carbon or nitrogen source and thus it should not
510 represent a contaminant for *in situ* applications, so that the effluent of the reactor does not need
511 any additional cleaning step before application for bioaugmentation.

512 Due to the substrate-specificity of reductive dehalogenases, sometimes it is inevitable to use
513 organohalides that are toxic or organohalides that produce toxic dehalogenated products. In
514 such cases, continuous cultivation of *Dehalococcoides* is still feasible with our reactor design,
515 as long as necessary precautions are taken. The pressure monitoring could even be applied when
516 volatile organohalides or products are involved, e.g., dechlorination from TCE to ethene. In
517 such cases, an adjustment to the H₂ consumption rate has to be made to compensate for partial
518 pressure increase that is caused by the production of the volatile compound (e.g., ethene). In
519 summary, the reactor setup presented in this study is broadly applicable to other
520 *Dehalococcoides* or *Dehalogenimonas* strains with organohalides other than brominated
521 tyrosines.

522 **5 Conclusions**

523 *D. mccartyi* strain CBDB1 was successfully cultivated in continuous mode in a semi-continuous
524 stirred tank reactor and long-term stable operation was achieved. Acetate, instead of
525 fermentable organics, was used as the carbon source. The simple and easy-handled design, the
526 feasibility of monitoring the dehalogenation process in real time, the reactor resilience to
527 confront high organohalide loading rates and the possibility of obtaining high cell density
528 cultures, make the CSTR a promising tool for stable cultivation.

529 Growth on the compound 3,5-dibromotyrosine which produces non-toxic tyrosine was
530 demonstrated and molar cell yields obtained were in the same range of those previously shown
531 for *D. mccartyi* strain CBDB1. The specific reductive dehalogenases CbdbA238 and
532 CbdbA1092 were expressed when using dibromotyrosine as electron acceptor.

533 The tandem CSTR-dibromotyrosine is a good choice for producing high volume of *D. mccartyi*
534 strain CBDB1 cultures at high biomass concentration, which can be used in downstream
535 processes, either for establishing bioremediation strategies in contaminated sites or for their
536 further use in research.

537 **Acknowledgements**

538 The authors thank Benjamin Scheer and Felicitas Ehme for technical support. C.R. was
539 financially supported by the European Union's Horizon 2020 research and innovation
540 programme under the Marie Skłodowska-Curie grant agreement No. 887923. Protein mass
541 spectrometry was done at the Centre for Chemical Microscopy (ProVIS) at the Helmholtz
542 Centre for Environmental Research - UFZ.

- 544 Adrian, L., Hansen, S.K., Fung, J.M., Görisch, H., Zinder, S.H., 2007a. Growth of
545 *Dehalococcoides* strains with chlorophenols as electron acceptors. *Environ. Sci.*
546 *Technol.* 41, 2318–2323. <https://doi.org/10.1021/es062076m>
- 547 Adrian, L., Manz, W., Szewzyk, U., Görisch, H., 1998. Physiological characterization of a
548 bacterial consortium reductively dechlorinating 1,2,3- and 1,2,4-trichlorobenzene.
549 *Appl. Environ. Microbiol.* 64, 496–503. [https://doi.org/10.1128/AEM.64.2.496-](https://doi.org/10.1128/AEM.64.2.496-503.1998)
550 503.1998
- 551 Adrian, L., Rahnenführer, J., Gobom, J., Hölscher, T., 2007b. Identification of a chlorobenzene
552 reductive dehalogenase in *Dehalococcoides* sp. strain CBDB1. *Appl. Environ.*
553 *Microbiol.* 73, 7717–7724. <https://doi.org/10.1128/AEM.01649-07>
- 554 Berggren, D.R.V., Marshall, I.P.G., Azizian, M.F., Spormann, A.M., Semprini, L., 2013.
555 Effects of sulfate reduction on the bacterial community and kinetic parameters of a
556 dechlorinating culture under chemostat growth conditions. *Environ. Sci. Technol.* 47,
557 1879–1886. <https://doi.org/10.1021/es304244z>
- 558 Cooper, M., Wagner, A., Wondrousch, D., Sonntag, F., Sonnabend, A., Brehm, M.,
559 Schüürmann, G., Adrian, L., 2015. Anaerobic microbial transformation of halogenated
560 aromatics and fate prediction using electron density modeling. *Environ. Sci. Technol.*
561 49, 6018–6028. <https://doi.org/10.1021/acs.est.5b00303>
- 562 Delgado, A.G., Fajardo-Williams, D., Popat, S.C., Torres, C.I., Krajmalnik-Brown, R., 2014.
563 Successful operation of continuous reactors at short retention times results in high-
564 density, fast-rate *Dehalococcoides* dechlorinating cultures. *Appl. Microbiol.*
565 *Biotechnol.* 98, 2729–2737. <https://doi.org/10.1007/s00253-013-5263-5>
- 566 Ding, C., Adrian, L., 2020. Comparative genomics in “*Candidatus Kuenenia stuttgartiensis*”
567 reveal high genomic plasticity in the overall genome structure, CRISPR loci and surface
568 proteins. *BMC Genomics* 21, 851. <https://doi.org/10.1186/s12864-020-07242-1>
- 569 Ding, C., Enyi, F.O., Adrian, L., 2018. Anaerobic ammonium oxidation (Anammox) with
570 planktonic cells in a redox-stable semicontinuous stirred-tank reactor. *Environ. Sci.*
571 *Technol.* 52, 5671–5681. <https://doi.org/10.1021/acs.est.7b05979>
- 572 Franke, S., Seidel, K., Adrian, L., Nijenhuis, I., 2020. Dual element (C/Cl) isotope analysis
573 indicates distinct mechanisms of reductive dehalogenation of chlorinated ethenes and
574 dichloroethane in *Dehalococcoides mccartyi* strain BTF08 with defined reductive
575 dehalogenase inventories. *Front. Microbiol.* 11:1507.
576 <https://doi.org/10.3389/fmicb.2020.01507>
- 577 Jayachandran, G., Görisch, H., Adrian, L., 2003. Dehalorespiration with hexachlorobenzene
578 and pentachlorobenzene by *Dehalococcoides* sp. strain CBDB1. *Arch. Microbiol.* 180,
579 411–416. <https://doi.org/10.1007/s00203-003-0607-7>
- 580 Kublik, A., Deobald, D., Hartwig, S., Schiffmann, C.L., Andrades, A., von Bergen, M., Sawers,
581 R.G., Adrian, L., 2016. Identification of a multi-protein reductive dehalogenase
582 complex in *Dehalococcoides mccartyi* strain CBDB1 suggests a protein-dependent
583 respiratory electron transport chain obviating quinone involvement. *Environ. Microbiol.*
584 18, 3044–3056. <https://doi.org/10.1111/1462-2920.13200>
- 585 Löffler, F.E., Yan, J., Ritalahti, K.M., Adrian, L., Edwards, E.A., Konstantinidis, K.T., Müller,
586 J.A., Fullerton, H., Zinder, S.H., Spormann, A.M., 2013. *Dehalococcoides mccartyi*
587 gen. nov., sp. nov., obligately organohalide-respiring anaerobic bacteria relevant to
588 halogen cycling and bioremediation, belong to a novel bacterial class, *Dehalococcoidia*
589 classis nov., order *Dehalococcoidales* ord. nov. and family *Dehalococcoidaceae* fam.
590 nov., within the phylum *Chloroflexi*. *Int. J. Syst. Evol. Microbiol.* 63, 625–635.
591 <https://doi.org/10.1099/ijs.0.034926-0>

592 Madigan, M.T., Martinko, J.M., Brock, T.D., 2006. Brock biology of microorganisms. Pearson
593 Prentice Hall, Upper Saddle River, NJ.

594 Maillard, J., Willemin, M.S., 2019. Regulation of organohalide respiration, Adv. Microb.
595 Physiol. Elsevier Ltd. <https://doi.org/10.1016/bs.ampbs.2019.02.002>

596 Mao, X., Stenuit, B., Tremblay, J., Yu, K., Tringe, S.G., Alvarez-Cohen, L., 2019. Structural
597 dynamics and transcriptomic analysis of *Dehalococcoides mccartyi* within a TCE-
598 Dechlorinating community in a completely mixed flow reactor. Water Res. 158, 146–
599 156. <https://doi.org/10.1016/j.watres.2019.04.038>

600 Marco-Urrea, E., Nijenhuis, I., Adrian, L., 2011. Transformation and carbon isotope
601 fractionation of tetra- and trichloroethene to trans-dichloroethene by *Dehalococcoides*
602 sp. strain CBDB1. Environ. Sci. Technol. 45, 1555–1562.
603 <https://doi.org/10.1021/es1023459>

604 Marco-Urrea, E., Seifert, J., von Bergen, M., Adrian, L., 2012. Stable isotope peptide mass
605 spectrometry to decipher amino acid metabolism in *Dehalococcoides* strain CBDB1. J.
606 Bacteriol. 194, 4169–4177. <https://doi.org/10.1128/JB.00049-12>

607 Mortan, S.H., Martín-González, L., Vicent, T., Caminal, G., Nijenhuis, I., Adrian, L., Marco-
608 Urrea, E., 2017. Detoxification of 1,1,2-trichloroethane to ethene in a bioreactor co-
609 culture of *Dehalogenimonas* and *Dehalococcoides mccartyi* strains. J. Hazard. Mater.
610 331, 218–225. <https://doi.org/10.1016/j.jhazmat.2017.02.043>

611 Rothery, R.A., Workun, G.J., Weiner, J.H., 2008. The prokaryotic complex iron–sulfur
612 molybdoenzyme family. Biochim. Biophys. Acta - Biomembr. 1778, 1897–1929.
613 <https://doi.org/10.1016/j.bbamem.2007.09.002>

614 Schipp, C.J., Marco-Urrea, E., Kublik, A., Seifert, J., Adrian, L., 2013. Organic cofactors in the
615 metabolism of *Dehalococcoides mccartyi* strains. Phil. Trans. R. Soc. B. 368,
616 20120321–20120321. <https://doi.org/10.1098/rstb.2012.0321>

617 Seidel, K., Kühnert, J., Adrian, L., 2018. The complexome of *Dehalococcoides mccartyi* reveals
618 its organohalide respiration-complex is modular. Front. Microbiol. 9, 1–14.
619 <https://doi.org/10.3389/fmicb.2018.01130>

620 Steffan, R.J., Schaefer, C.E., 2016. Current and future bioremediation applications:
621 bioremediation from a practical and regulatory perspective, in: Adrian, L., Löffler, F.E.
622 (Eds.), Organohalide-Respiring Bacteria. Springer Berlin Heidelberg, Berlin,
623 Heidelberg, pp. 517–540. https://doi.org/10.1007/978-3-662-49875-0_22

624 Wagner, A., Cooper, M., Ferdi, S., Seifert, J., Adrian, L., 2012. Growth of *Dehalococcoides*
625 *mccartyi* strain CBDB1 by reductive dehalogenation of brominated benzenes to
626 benzene. Environ. Sci. Technol. 46, 8960–8968. <https://doi.org/10.1021/es3003519>

627 Yang, C., Kublik, A., Weidauer, C., Seiwert, B., Adrian, L., 2015. Reductive dehalogenation
628 of oligocyclic phenolic bromoaromatics by *Dehalococcoides mccartyi* strain CBDB1.
629 Environ. Sci. Technol. 49, 8497–8505. <https://doi.org/10.1021/acs.est.5b01401>

630 Zhuang, W.-Q., Yi, S., Bill, M., Brisson, V.L., Feng, X., Men, Y., Conrad, M.E., Tang, Y.J.,
631 Alvarez-Cohen, L., 2014. Incomplete Wood–Ljungdahl pathway facilitates one-carbon
632 metabolism in organohalide-respiring *Dehalococcoides mccartyi*. Proc. Natl. Acad. Sci.
633 111, 6419–6424. <https://doi.org/10.1073/pnas.1321542111>

634 Zinder, S.H., 2016. The Genus *Dehalococcoides*, in: Adrian, L., Löffler, F.E. (Eds.),
635 Organohalide-Respiring Bacteria. Springer Berlin Heidelberg, Berlin, Heidelberg, pp.
636 107–136. https://doi.org/10.1007/978-3-662-49875-0_6

637

638 **Figure Legends**

639 **Figure 1.** Performance of the CSTR during the different periods of operation in regard to the
640 L-3,5-dibromotyrosine (DBT) loading rate and the specific removal rate achieved. The
641 concentration of L-DBT in the CSTR is also presented. Period I and II correspond to reactor
642 operations using an influent with 5 mM of L-DBT and 1 liter of reactor volume. Period III to
643 VI correspond to reactor operations using an influent with 1 mM of L-DBT and 80 mL of
644 reactor volume. Units in nkat per cell refer to nmol of dibromotyrosine removed per second per
645 cell.

646 **Figure 2.** Reactor headspace pressure change (in gas volume equivalent) during a three-day
647 period (day 27-day 29 of the pre-reactor) of continuous operation using medium containing 5
648 mM D-DBT. Pressure increase at 29 h and 53 h was due to addition of 10 mL H₂ into the
649 headspace. The periodical short-term drop and rise in pressure were due to the regular operation
650 of the pump replacing 5 mL of culture liquid with 5 mL of fresh medium.

651 **Figure 3.** Cell density in the CSTR during the different periods of operation.

652 **Figure 4.** Average molar growth yield calculated for Periods III and IV (doubling time of 8 and
653 6 days, respectively) and Periods V and VI (doubling time of 4 and 3 days, respectively). **
654 denote *p* value < 0.01 in a t-test.

655 **Figure 5.** A) Epifluorescence microscopic image of the cells from the CSTR culture after
656 SYBR Green-staining; B) DGGE profile of bacterial DNA extracted from the CSTR culture
657 (lanes 1 and 5) and from three different pure or mixed batch cultures of our lab (lanes 2, 3 and
658 4). Lane 1 and 5 correspond to 2 months and 3 months operation time of the reactor,
659 respectively, on L-DBT. Cut and sequenced bands are indicated by black triangles; C)
660 Sequencing results of selected DGGE bands from the DGGE profiles. (* denote that sequences
661 did not show a significant similarity in BLAST; ** denote that the sequence retrieved from the
662 sequencing process was of poor quality).

Fig. 1

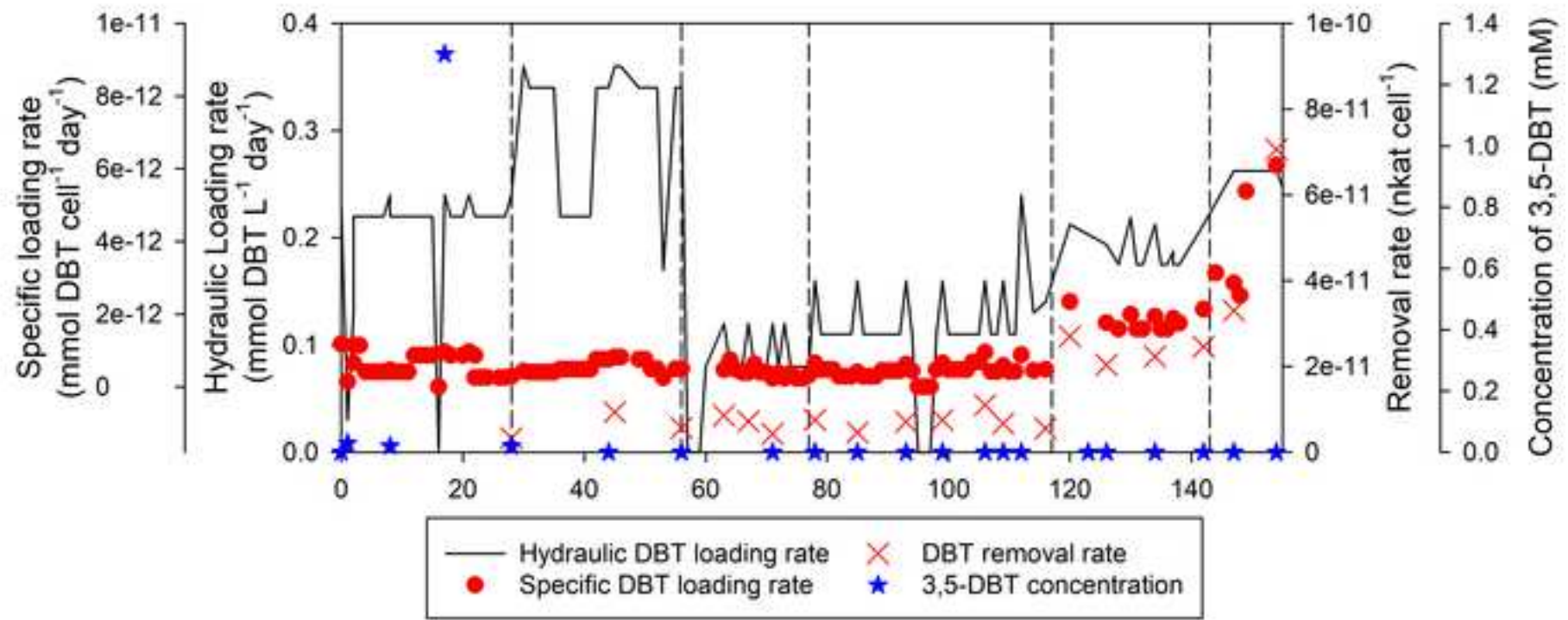


Fig. 2

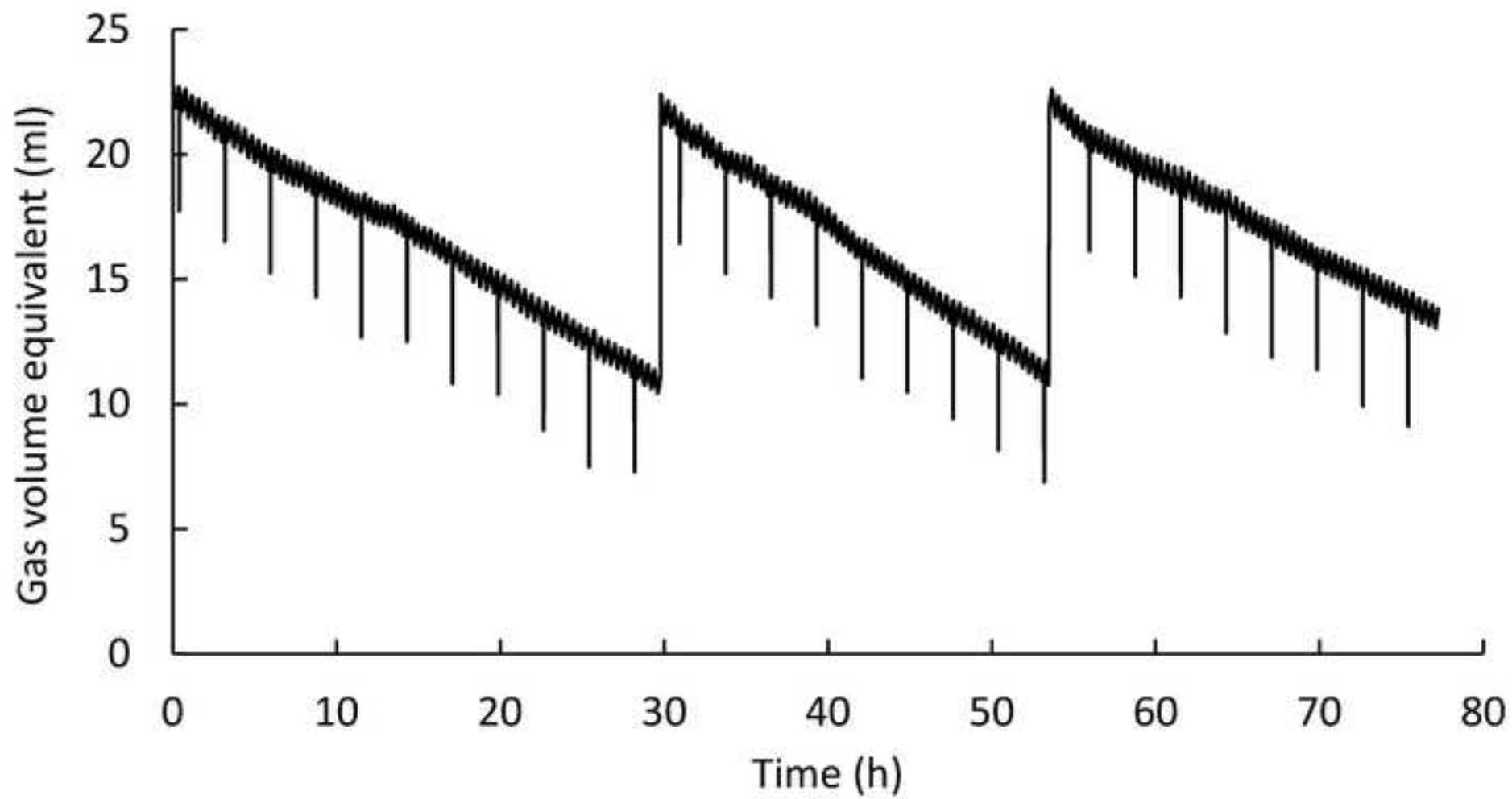


Fig. 3

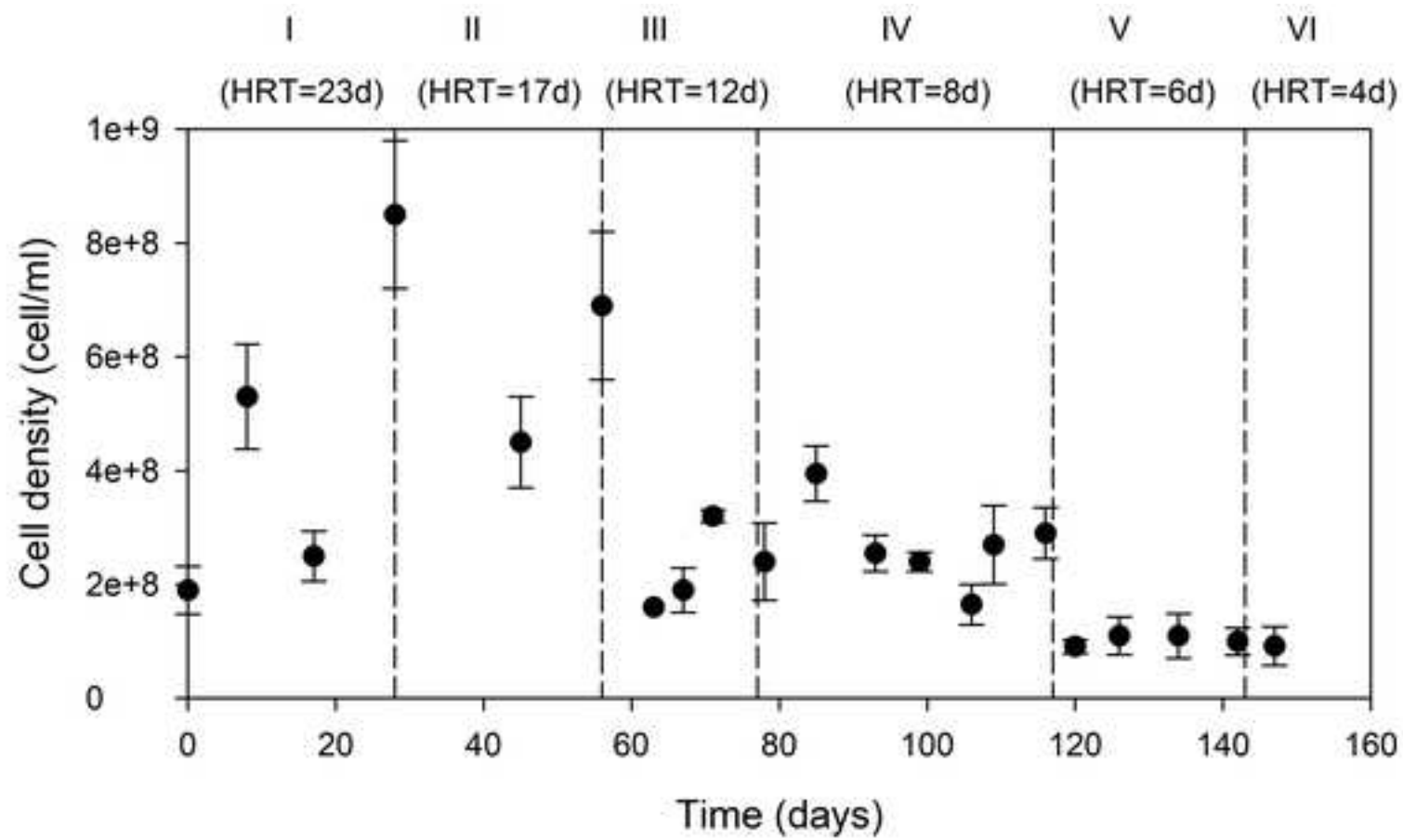
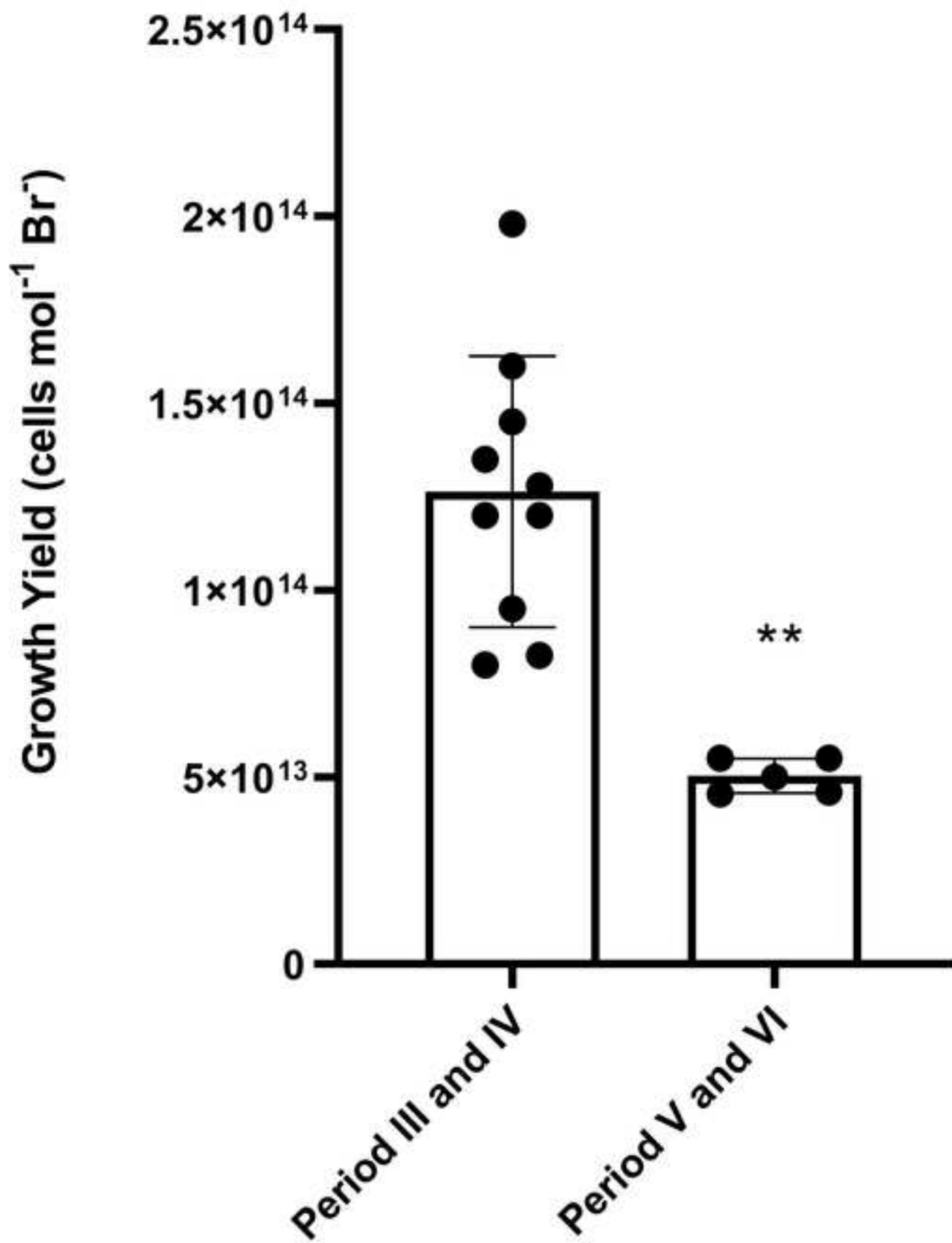


Fig. 4



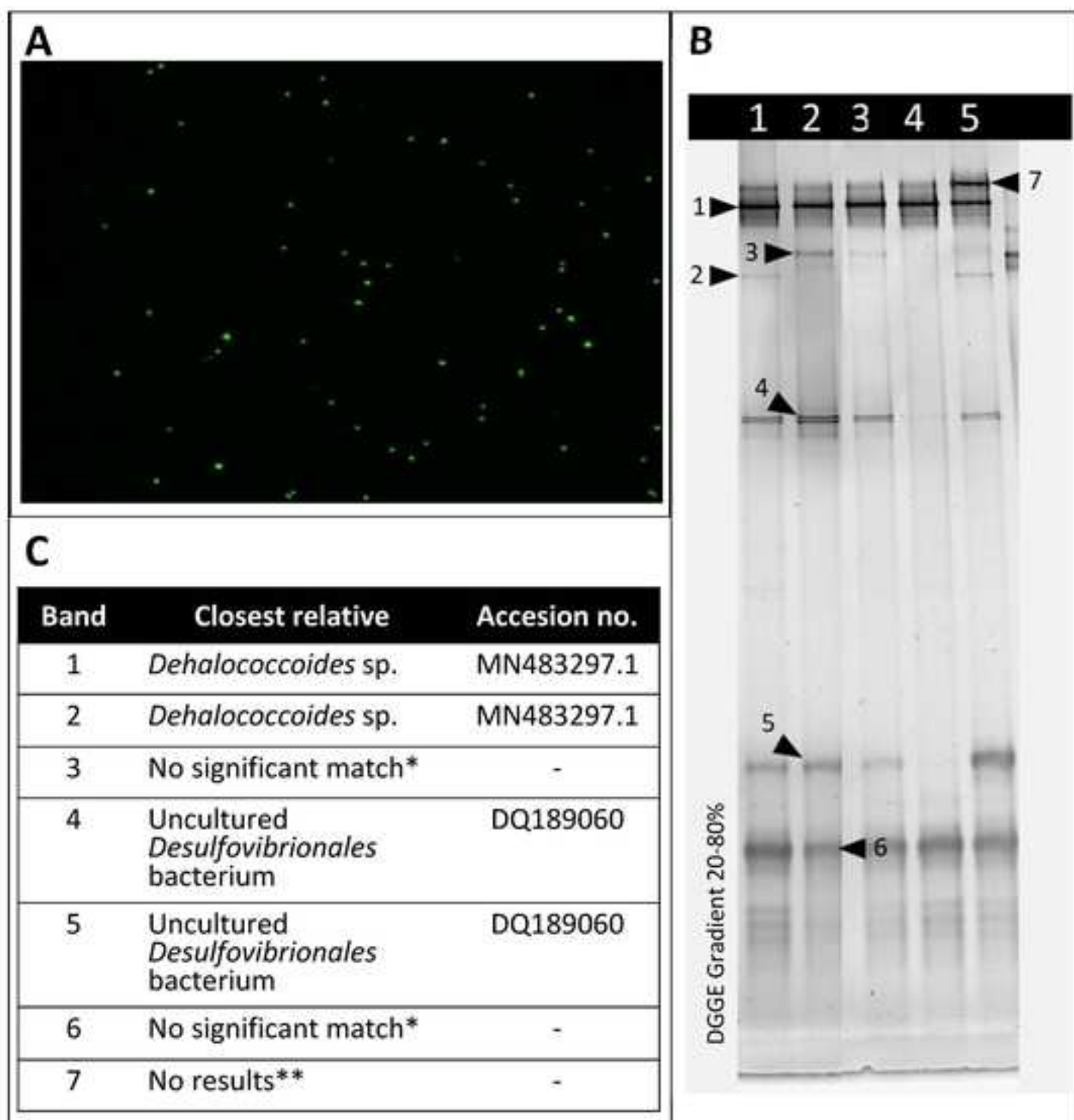


Table 1 Calculation of consumption of D-3,5-dibromotyrosine (D-DBT) and hydrogen in the headspace based on the dataset shown in Figure 3.

Calculation of D-DBT consumption		Calculation of hydrogen consumption	
D-DBT concentration in medium	5 mM	Gas consumed based on pressure change	31.3 mL
Medium added	140 mL (28 cycle \times 5 mL per cycle)	Compensation due to pH change (approximate)	5.7 mL (pH dropped from 6.8 to 6.6, therefore CO ₂ % increased from 7.4% to 9.9%, headspace volume 230 mL)
Total DBT added	0.70 mmol	Total H ₂ consumed	37.0 mL (at 30 °C), or 1.49 mmol
Theoretical H ₂ needed	1.40 mmol		

Table 2 Relative abundance (%) for the reductive dehalogenases (RdhA) identified by nLC-MS/MS analysis in strain CBDB1 culture fed with different halogenated compounds from previous works and from the work of the current study with dibromotyrosines. The pre-reactor was amended with D-3,5-dibromotyrosine (D-DBT), while the other 3,5-dibromotyrosine samples correspond to the reactor fed with L-3,5-dibromotyrosine (L-DBT).

RdhA	Chloro- and bromobenzenes							3,5-dibromotyrosine						Other phenolic compounds						
	TeBB	TeBB	TeBB (1)	HBB (2)	HCB (1)	HCB_1st	HCB_2nd	HCB_3rd	Pre-	Day 8	Day 21	Day 57	Day 112	Day 144	TBBPA	BPB (2)	BPB_1st	BPB_2nd	BPB_3rd	BPB_4th
CbdbA80	0.2			*	*		3.8	13					0.1		*	*				
CbdbA84	0.2	6.1	*	*	*		1.5	1.7	0	0	0.1	0	4.3	0.3	*		0.2			
CbdbA88					*															
CbdbA238									0.9	0.7	1.8	4.6	1.6	0.8						
CbdbA1092									2.6	2.7	0.9	0.4	11	15	*	*	0.1	0.1	0.5	0.2
CbdbA1453			*	*	*		0								*					
CbdbA1455				*	*				0	0.1		0			*	*	0			
CbdbA1503															*	*				
CbdbA1588			*		*		0													
CbdbA1595									0		0.1									
CbdbA1598							0.2													
CbdbA1618			*	*	*				0.1	0	0.1	0		0.3	*	*				
CbdbA1624											0.1	0		0.1						
CbdbA1638					*				0.1	0.1	0.1	0.1		0.2						

Note:

(1) Seidel et al. 2018 *Frontiers Microbiol*

(2) Yang et al. 2015 *ES&T*

* indicating presence of an RdhA at non-quantifiable abundance